MNRAS **473,** 5630–5640 (2018)
Advance Access publication 2017 October 25
doi:10.1093/mnras/stx2769

The evolution of photoevaporating viscous discs in binaries

Giovanni P. Rosotti★ and Cathie J. Clarke
Institute of Astronomy, University of Cambridge, Madingley Rd, Cambridge CB3 0HA, UK

Accepted 2017 October 23. Received 2017 October 14; in original form 2017 April 13

ABSTRACT

A large fraction of stars are in binary systems, yet the evolution of protoplanetary discs in binaries has been little explored from the theoretical side. In this paper, we investigate the evolution of the discs surrounding the primary and secondary components of binary systems on the assumption that this is driven by photoevaporation induced by X-rays from the respective star. We show how for close enough separations (20–30 au for average X-ray luminosities) the tidal torque of the companion changes the qualitative behaviour of disc dispersal from inside out to outside in. Fewer transition discs created by photoevaporation are thus expected in binaries. We also demonstrate that in close binaries the reduction in viscous time leads to accelerated disc clearing around both components, consistent with *unresolved* observations. When looking at the *differential* disc evolution around the two components, in close binaries discs around the secondary clear first due to the shorter viscous time-scale associated with the smaller outer radius. In wide binaries instead the difference in photoevaporation rate makes the secondaries longer lived, though this is somewhat dependent on the assumed scaling of viscosity with stellar mass. We find that our models are broadly compatible with the growing sample of *resolved* observations of discs in binaries. We also predict that binaries have higher accretion rates than single stars for the same disc mass. Thus, binaries probably contribute to the observed scatter in the relationship between disc mass and accretion rate in young stars.

Key words: accretion, accretion discs – protoplanetary discs – circumstellar matter – stars: pre-main-sequence.

1 INTRODUCTION

A large fraction of stars are in binary systems (Raghavan et al. 2010). Despite the possible impediments to planet formation in binaries (Thebault 2011; Marzari et al. 2013; Rafikov 2013; Lines et al. 2015), the growing census of planets discovered in binary systems attests to the fact that planet formation is indeed viable in these environments, either around one of the two components (e.g. Hatzes et al. 2003; Dumusque et al. 2012) or around the binary itself (Doyle et al. 2011; Welsh et al. 2012). In addition, planet formation is likely to be affected by the influence of binarity on disc lifetime and this has spurred a number of observational efforts to characterize the disc bearing properties of stars in young binaries (e.g. Cieza et al. 2009; Daemgen, Correia & Petr-Gotzens 2012; Kraus et al. 2012; Daemgen et al. 2013).

Such surveys offer a broader opportunity to test our understanding of protoplanetary disc evolution. Disc evolution is widely modelled (Clarke, Gendrin & Sotomayor 2001; Alexander, Clarke & Pringle 2006; Owen, Ercolano & Clarke 2011) in terms of parametrized viscous evolution which is terminated when such evolution becomes dominated by photoevaporation by the central star. Such models, as applied to single stars, have been shown to be compatible with a wide range of observed diagnostics, such as the evolution of the disc fraction with time (e.g. Haisch, Lada & Lada 2001; Fedele et al. 2010; Ribas et al. 2014), and naturally provide an explanation for at least some transition discs (Owen & Clarke 2012), i.e. discs that show evidence for an inner hole; such models have not however been tested in binary systems. In this paper, we test whether such models are consistent with the available data on discs in binary systems, drawing both on resolved observations (where the presence of discs around individual components is detected, e.g. Daemgen et al. 2012, 2013) and unresolved observations (which instead indicate the presence of a disc in at least one member of the pair, e.g. Cieza et al. 2009; Kraus et al. 2012).

There are two distinct differences that apply to discs in binaries, which can be used to our advantage. First, binary components are coeval to an excellent approximation. Theoretically, the only viable scenario for binary formation is the fragmentation of a molecular cloud core (see Reipurth et al. 2014 for a recent review on the subject), which implies a difference in age of up to $\sim 10^5$ yr (the free-fall time of the natal core), a small fraction of the typical ages of T Tauri stars. This coevality has been confirmed in a number of systems by placing components on pre-main-sequence tracks (Kraus &

★ E-mail: rosotti@ast.cam.ac.uk

Hillenbrand 2009): indeed Daemgen et al. (2012) confirmed coevality in all cases where low veiling permits an accurate age calibration (see also the review of Stassun, Feiden & Torres 2014). This is in contrast to the situation within star-formation regions where age spreads may be large and are poorly quantified (see e.g. Palla & Stahler 2000; Hillenbrand, Bauermeister & White 2008; Jeffries et al. 2011). The coeval nature of binary components then makes it possible to study disc evolution as a function of stellar mass. Secondly, the disc outer radius is well constrained in binary systems by the tidal effect of the companion star: this imposes a zero mass flux outer boundary to the disc at a radius that is a dynamically determined function of binary mass ratio and separation (Papaloizou & Pringle 1977; Pichardo, Sparke & Aguilar 2005; see also the observational study of Harris et al. 2012). In discs whose evolution is driven by accretion on to the star, the evolution time-scale at all radii in the disc is given by the viscous time-scale at the disc's outer edge (Pringle 1981), and it is a significant disadvantage that this quantity is not well constrained observationally in single stars. The well-defined outer radius of a binary provides a laboratory to study the dependence of the viscous time-scale on radius.

In this paper, we assume that disc dispersal is driven by X-ray photoevaporation. This is motivated by the fact that the dependence of X-ray luminosity (and hence photoevaporation rate) is well quantified as a function of stellar mass (see Preibisch et al. 2005; Güdel et al. 2007) which is a necessary ingredient when examining differential disc lifetimes in binaries. Modelling photoevaporation by EUV radiation is complicated by the fact that the EUV luminosity of T Tauri stars (and its mass dependence) is not well constrained observationally (Alexander, Clarke & Pringle 2005), while FUV photoevaporation (Gorti & Hollenbach 2009) by the central star has not yet been subject to radiation hydrodynamical modelling. In the X-ray case, mass-loss rates vary roughly linearly with X-ray luminosity and, as noted above, give rise to models of single star disc evolution that are broadly compatible with observations.

This paper is organized as follows. Section 2 introduces the model we use to describe disc evolution and Section 3 presents our results about disc evolution. We then compare our results with the observations in Section 4 and we finally draw our conclusions in Section 5.

2 DESCRIPTION OF THE MODEL

We assume that the discs surrounding each star within a binary system evolve independently. Strictly speaking this means that our calculation is only applicable to the phase of disc evolution when re-supply of gas from beyond the binary orbit can be neglected. Empirically, this is motivated by the absence of substantial circumbinary discs in most binaries that are wider than a few au (e.g. Jensen, Mathieu & Fuller 1996; see also the discussion in Monin et al. 2007).

We also assume that the photoevaporation of each disc is dominated by the wind driven by the X-ray luminosity of its respective central star, i.e. that there is no cross-over of X-ray heating between discs. This is likely to be a good approximation for binaries whose separation exceeds the radius in the disc (R_X) within which X-ray photoevaporation is effective: R_X is about 80 au for a solar mass star and scales linearly with stellar mass (Owen, Clarke & Ercolano 2012). For closer binaries, there is some possibility of cross-over, although this cannot be quantified without three-dimensional simulations. Nevertheless, this omission is unlikely to affect any of our conclusions: it will only be significant in the case of close, extreme mass ratio binaries, in which case the extra flux from the X-ray luminous primary may accelerate the clearing of the secondary's disc. This is however a regime in which the secondary's disc in any case clears significantly faster than the primary's by purely viscous processes.

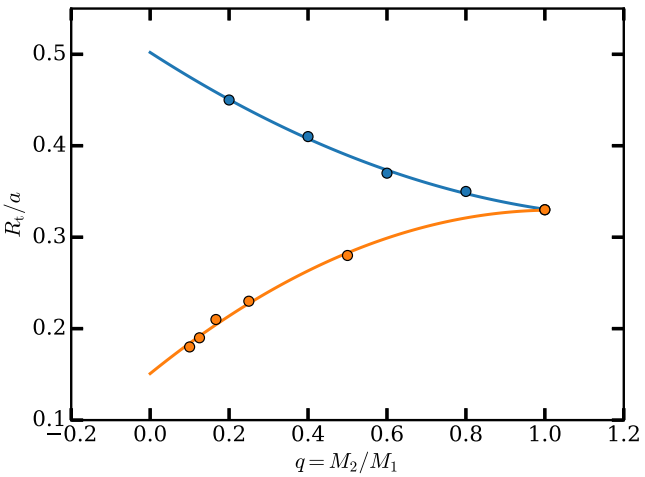

Figure 1. The tidal radii of the primary/secondary discs (upper and lower curves) normalized to the binary separation as a function of binary mass ratio, $q = M_2/M_1$. Data points from Papaloizou & Pringle (1977), while the curves are the numerical fits employed in this work.

2.1 Method

For a binary of given component masses (M_1 and M_2), mass ratio q ($=M_2/M_1$) and separation, a, the tidal truncation radius, R_t, of each disc is calculated using the formula given in Papaloizou & Pringle (1977, see Fig. 1). Note that for a mass ratio of unity this produces the well-known result that the truncation radius $R_t \simeq a/3$. The initial mass of each disc is assigned a value equal to $0.1\times$ the mass of its parent star; this is distributed with a surface density profile:

$$\Sigma(R, 0) = \frac{C}{R}\exp\left(-\frac{\mathrm{R}}{\mathrm{R_1}}\right), \quad (1)$$

where C is adjusted to give the correct disc mass within a radius R_t.[1] Our initial conditions correspond to a viscous similarity solution (Lynden-Bell & Pringle 1974; Hartmann et al. 1998) for a freely expanding disc with kinematic viscosity $\nu \propto R$ (see below) and was the functional form adopted by Owen et al. (2010, with $R_1 = 18$ au, which we assume in this work) as a plausible initial condition that matched the resulting model properties to observed discs in single stars. Note that this initial distribution (and its dependence on stellar mass) is poorly constrained observationally. The $\Sigma \propto R^{-1}$ dependence (for $R < R_1$) is motivated by the observed power-law decline in disc surface density inferred from mm imaging (Williams & Cieza 2011); in the absence of information about the scaling of viscosity with stellar mass (cf. Alexander & Armitage 2006; Dullemond, Natta & Testi 2006), we set the viscosity law as $\nu = \nu_0(R/R_0)$ where the value $\nu_0/R_0 = 10^{-5}$ au yr^{-1} yields observationally reasonable disc lifetimes of order a few Myr (Haisch et al. 2001; Fedele et al. 2010).

[1] We have checked that the results are not significantly changed if C is adjusted so that 10 per cent of the stellar mass instead corresponds to the total mass the disc would have out to infinite radius.

X-ray photoevaporation is included by applying the parametrization of X-ray mass-loss per unit area ($\dot{\Sigma}_{\rm X}$) given in Owen et al. (2012) The mass-loss profile has the property that the radial scaling is proportional to stellar mass, that is,

$$\dot{\Sigma}_{\rm X} = \dot{\Sigma}_{\rm X}(RM_*^{-1}), \tag{2}$$

while the total wind loss mass rate scales linearly with the X-ray luminosity.

The X-ray luminosity of T Tauri stars has been well characterized by the Chandra Orion Ultra-deep Project (Preibisch et al. 2005; see also Güdel et al. 2007 for similar results obtained using *XMM* in Taurus). In Section 3, we assign X-ray luminosities to stellar mass using the mass dependence of the *mean* X-ray luminosity i.e. $L_{\rm X} \propto M_*^{1.44}$; we note however that the scatter is large (standard deviation, σ, in $\log_{10}(L_{\rm X})$ of 0.65) at all masses and in Section 4 we undertake population synthesis in which we select X-ray luminosities from a mass-dependent luminosity function with this σ.

The model discs are evolved through integration of the viscous diffusion equation:

$$\frac{\partial \Sigma}{\partial t} = \frac{1}{R}\frac{\partial}{\partial R}\left[3R^{1/2}\frac{\partial}{\partial R}(\nu \Sigma R^{1/2})\right] - \dot{\Sigma}_{\rm X} \tag{3}$$

and the presence of the companion is modelled by imposing a zero flux boundary condition ($\partial(\nu\Sigma R^{1/2})/\partial R = 0$) at $R = R_{\rm t}$, as commonly employed in the context of evolved binaries such as dwarf novae (e.g. Bath & Pringle 1981) and justified by the fact that the tidal torque from the companion has a very steep dependence on radius. In practice, this means that its action is restricted to a very narrow region and our approach is equivalent to assuming that the affected region is infinitesimally thin. This is often called a closed boundary condition in the context of the theory of differential equations. Equation (3) is differenced on a grid equispaced in $R^{1/2}$ and the equation is integrated via a standard finite-difference method, first-order accurate in time and second-order accurate in space (Pringle, Verbunt & Wade 1986); the code is described in detail in Ercolano & Rosotti (2015).

3 RESULTS: THE EVOLUTION OF PHOTOEVAPORATING VISCOUS DISCS IN BINARIES

3.1 The effect of tidal truncation on disc evolution

In this section, we address how the evolution of a *single* disc around one of the two components of the binary is affected by the closed boundary imposed by the tidal torque of the companion.

3.1.1 Qualitative behaviour

In the case of discs around single stars, the interplay between photoevaporation and viscous evolution produces a well-defined evolutionary sequence (Clarke et al. 2001; Owen et al. 2010): (a) a prolonged phase of viscous draining that is little modified by the photoevaporative mass-loss (b), a phase of so-called photoevaporation starved accretion (Drake et al. 2009) where the disc profile becomes somewhat depleted in the region of maximum mass-loss (i.e. at tens of au), (c) the opening of a gap in the disc at a point where the mass-loss rate starts to decline steeply (i.e. at a few au), (d) the viscous draining of the inner disc and (e) the progressive erosion of the outer disc by photoevaporation. During the last phase (e) [and possibly during phase (d)], see Alexander & Armitage (2007), the disc has an inner hole and is therefore a transition disc.

In the binary case, phase (a) is modified after significant material has diffused out to interact with the tidal boundary condition at $R_{\rm t}$. From this point (in the absence of photoevaporation), the disc would evolve towards a similarity solution that differs from that which applies in the case of a freely expanding disc (Lynden-Bell & Pringle 1974):

$$\Sigma(R,t) = \Sigma_0 \frac{R_1}{R}(1+t/t_{\nu,1})^{-3/2}\exp\left(-\frac{R}{R_1(1+t/t_{\nu,1})}\right). \tag{4}$$

The solution of equation (3) with a closed outer boundary and no photoevaporation can be obtained via separation of variables and is instead

$$\Sigma(R,t) = \frac{A}{R^{3/2}}\sin\left(\frac{\pi R^{1/2}}{2R_{\rm t}^{1/2}}\right)\exp\left(-\frac{t}{t_{\rm t}}\right), \tag{5}$$

as can be verified by substitution into equation (3), where $t_t = 16R_{\rm t}^2/3\pi^2\nu_t$, ν_t is the kinematic viscosity at $R_{\rm t}$ (i.e. $\nu_0 R_{\rm t}/R_0$) and A and Σ_0 are normalization constants. Note that, while in both similarity solutions $\Sigma \propto R^{-1}$ at small radii, the closed boundary condition leads to a power law of index -1.5 in the outer regions of the disc.

We find that the qualitative sequence of photoevaporative/viscous clearance that we outlined above as (a)–(e) is also followed in the binary case provided $R_{\rm t}$ is significantly larger than the location of gap opening; in practice this means cases where $R_{\rm t} > R_{\rm crit} \sim 20(M/{\rm M}_\odot)$ au, although $R_{\rm crit}$ can be as large as 100 au for the highest X-ray luminosities. The upper panel of Fig. 2 depicts the evolution of the surface density profile in such a case.

For discs with $R_{\rm t} < R_{\rm crit}$ (see above), an inner hole never forms. The middle panel of Fig. 2 shows the time evolution of such a disc. While a gap does open in the disc, the mass that would normally be in the region between the gap and the outer radius of the disc contains little mass and photoevaporation removes it before the inner disc drains on to the star. In other words, phase (e) goes to completion before phase (d). Once photoevaporation has removed the outer disc, the subsequent clearing of the inner disc proceeds from outside in.

For even smaller $R_{\rm t}$ ($\lesssim$ a few au), the location of gap opening is outside the disc and therefore a gap never opens (see lower panel of Fig. 2). In this case, the disc clears purely from outside in.

Fig. 3 shows the range of parameters for which inner holes do (blue dots) and do not (orange crosses) form for stars with average X-ray luminosity $L_{\rm X} = 2.3 \times 10^{30}(M_*/{\rm M}_\odot)^{1.44}\,{\rm erg\,s^{-1}}$. On the x-axis, we plot the tidal truncation radius of the disc according to the formula shown in Fig. 1; the value depends on the combination of both the mass ratio and the binary separation. It can be seen how the $R_{\rm crit}$ dividing the discs that form holes from the ones that do not depends on the stellar mass, because of the radial scaling of the mass-loss profile (see equation 2).

3.1.2 Disc lifetime

We have shown that, if $R_{\rm t} > R_{\rm crit}$, photoevaporation creates inner holes (just as in single stars) and these may be identified with (at least some) observed transition discs (Owen & Clarke 2012; Owen et al. 2012). This does not mean however that the effect of the companion is completely negligible, and both the *absolute*

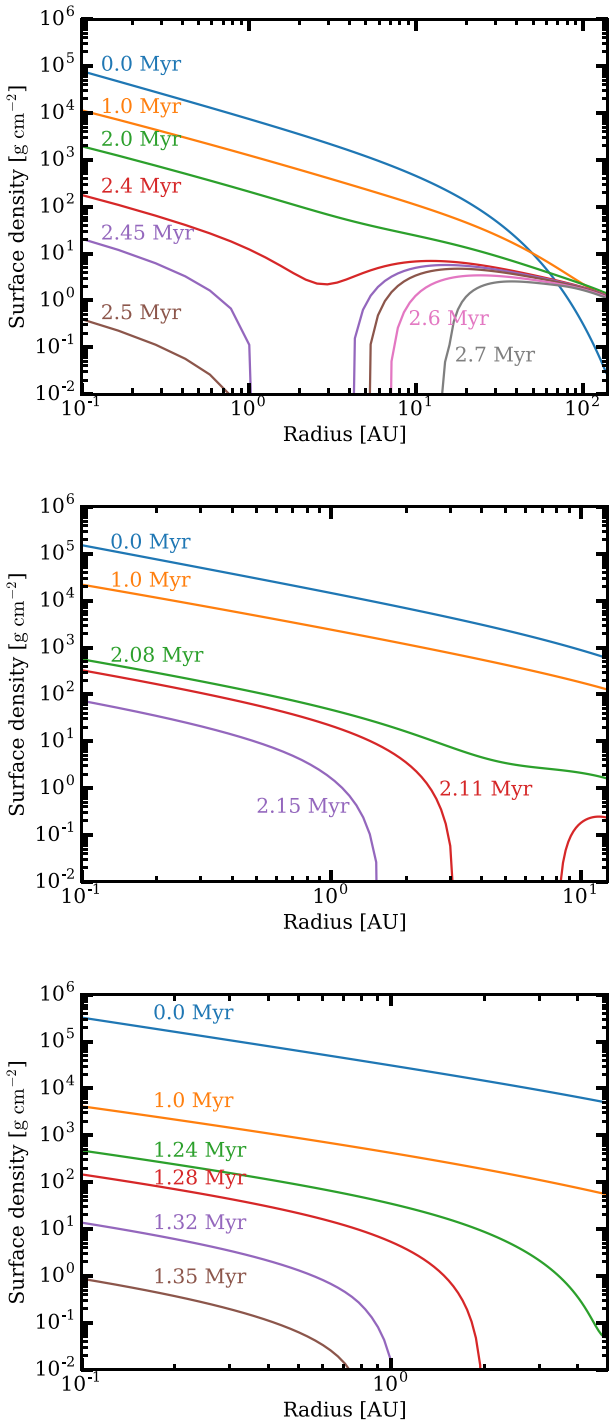

Figure 2. The main patterns of photoevaporative disc clearing in binaries identified in this paper. We plot snapshots of the surface density at selected times (indicated on the plot) for models with $M = 1\,\mathrm{M}_\odot$ and $L_\mathrm{X} = 2.3 \times 10^{30}\,\mathrm{erg\,s^{-1}}$. Upper panel: tidal radius of 140 au. The clearing sequence (with a gap forming at a few au) is similar to that seen in discs around single stars. Middle panel: an example of a disc that does not form an inner hole in a model with a tidal radius of 13 au. The disc develops a gap and the outer part of the disc is removed by photoevaporation. Subsequently the inner disc is cleared from outside in. Lower panel: a disc clearing purely outside in (without any gap) in a model with a tidal radius of 5 au.

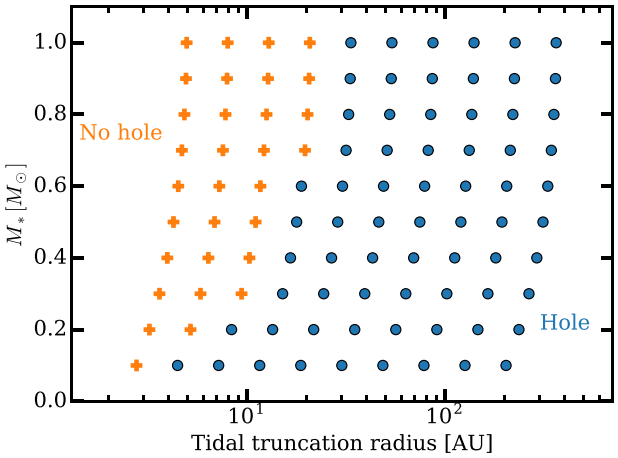

Figure 3. The regions of parameter space (stellar mass versus tidal truncation radius) for which inner holes form (blue circles) or not (green crosses) for average X-ray luminosity $L_\mathrm{X} = 2.3 \times 10^{30}(M_*/\mathrm{M}_\odot)^{1.44}\,\mathrm{erg\,s^{-1}}$.

lifetime[2] of the disc and the *fractional* time spent with an inner hole (transition disc) can be modified.

In single stars, the lifetime of a disc against photoevaporation is set by the time that is required for the viscous accretion rate in the disc to decline to the level of the photoevaporative mass-loss rate. According to the viscous similarity solution (equation 4), the accretion rate in a freely expanding disc declines as

$$\dot{M} = \dot{M}_\mathrm{in}(1 + t/t_{\nu 1})^{-1.5}, \tag{6}$$

where $t_{\nu 1}$ is the viscous time-scale at R_1 and $\dot{M}_\mathrm{in}$ is the initial accretion rate through the disc (which is proportional to the initial disc mass divided by $t_{\nu 1}$). In practice, the disc lifetime is thus set by the initial mass of the disc, its viscous evolution time-scale and the rate of photoevaporation. In the case of a disc in a binary, the value of R_t (which is a function of q and a) is also relevant (see Armitage, Clarke & Tout 1999). As discussed previously, after a time t_boundary that depends on the initial conditions and on the magnitude of the viscosity, the disc spreads enough to interact with the outer boundary, and from that time on according to equation (5) the mass accretion will decrease as

$$\dot{M}(t) = \dot{M}(t_1)\exp\left(-\frac{3\nu_0\pi^2 t}{16R_\mathrm{t}^2}\right), \tag{7}$$

which decays in an exponential fashion with time, with a time-scale that is the viscous time-scale t_t at the outer edge. Therefore, even in the absence of photoevaporation, discs with a small enough outer radius will clear[3] in 2–3 t_t. The presence of photoevaporation further hastens disc dispersal. We thus expect the disc lifetime to depend strongly on the value of R_t.

This expectation is borne out by Fig. 4, which illustrates the dependence of the lifetime on the outer disc radius. Indeed, while for large outer radii ($\gtrsim$100 au) there is little difference compared to a single star, for smaller radii the lifetime decreases dramatically. Fig. 4 shows also the dependence of the relative time spent as a

[2] 'Lifetime' is here defined as the time taken for the disc to clear out to the smaller of R_t and 100 au.

[3] This does not take into account the initial expansion up to R_t. In practice, we note that this happens on a time-scale smaller or comparable to t_t and thus does not change significantly the estimate.

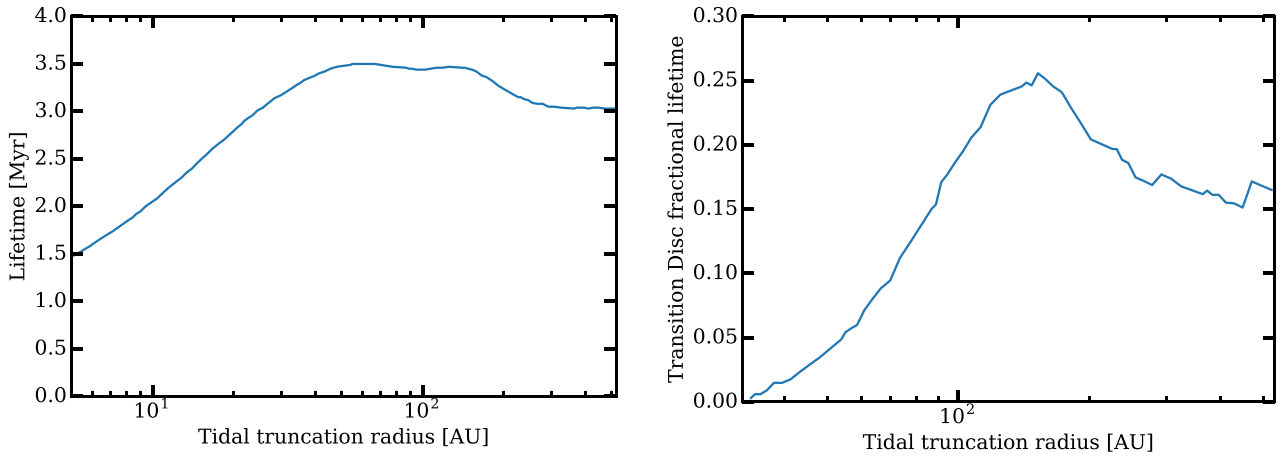

Figure 4. Lifetimes as a function of the disc outer radius, set by the tidal forces of the companion. Both cases are for a star with $M = 1\,\mathrm{M}_\odot$ with average X-ray luminosity ($L_\mathrm{X} = 2.3 \times 10^{30}\,\mathrm{erg\,s^{-1}}$). Left-hand panel: total lifetime of the disc. Right-hand panel: fraction of the lifetime spent as a transition disc.

transition disc (i.e. phases d–e). For radii smaller than ∼100 au, the fraction decreases and eventually vanishes for radii of ∼40 au, at which point the qualitative behaviour of the evolution switches to outside-in clearing (see previous section). The reason for the reduction in the fraction spent as a transition disc is that after gap opening the bulk of the remaining disc is retained in the region where the photoevaporation is concentrated and also that the disc in this region follows the steeper ($\Sigma \propto R^{-1.5}$) profile imposed by the binary boundary condition, and therefore less mass is present outside the gap. Thus, although inner holes can form in binaries, their incidence should be lower than in single stars for outer radii smaller than 100 au, corresponding to binary separations less than ∼300 au. Observationally, this means that we expect a smaller fraction of transition discs in binaries with a separation smaller than 300 au. The fraction of transition discs in binaries is currently poorly quantified, but it is interesting to note that the transition disc catalogue of van der Marel et al. (2016) reports only four transition discs in binaries,[4] out of a sample of ∼150 objects.

3.1.3 Summary

While disc clearing in wide binaries ($\gtrsim$30 au) proceeds in a similar fashion to single stars, the lifetime of transition discs is expected to decline somewhat for close enough separations ($\lesssim$100 au) as it becomes easier for photoevaporation to rapidly remove the remnant outer disc. For closer binaries ($\lesssim$30 au), we do not expect photoevaporation to create a hole but instead to produce progressive clearance of the disc from the outside in. We stress that these estimates are based on a particular assumption about the radial dependence of the kinematic viscosity ($\nu \propto R$) and that the detailed predictions would be expected to change in the case of a more realistic viscosity model.

[4] We have excluded objects that are compatible with being circumbinary discs since in this paper we only study discs around each of the two components. Our final list comprises the following objects: 2MASS J04303235+3536133, 2MASS J04304004+3542101, 2MASS J04292165+2701259 and 2MASS J16274028−2422040.

3.2 The differential evolution of discs within binary star systems

In this section, we now turn to consider the *differential* evolution of the discs around both components of the binary, highlighting in particular the dependence on the stellar mass. We have shown in the previous section that the disc lifetime is set by the initial mass of the disc and its viscous evolution time-scale, as well as by the rate of photoevaporation. We have also shown the dependence on the disc outer radius R_t, which is a function of q and a. On these grounds, discs around secondaries should be expected to clear more rapidly on average because their discs are smaller (cf. Fig. 1); Armitage et al. (1999) noted that this should imply a significant fraction of binaries in which only the primary was associated with a disc (i.e. CW pairs in the notation of Monin et al. 2007, where C refers to the Classical T Tauri star status of disc possessing stars, W designates Weak Line (disc-less) T Tauri stars and the ordering refers to the primary and secondary, respectively). However, additional factors are involved when photoevaporation is included: the mean X-ray luminosity (and hence wind photoevaporation rate) scales as $M_*^{1.44}$ compared with the assumed linear scaling of the initial disc mass with stellar mass: on these grounds, one would expect the disc of the secondary star to be longer lived and might thus expect the preferential production of WC pairs.

Fig. 5 shows that both these effects come into play, depending on the binary separation. For closer binaries, the disc is able to viscously diffuse out to R_t before the discs are significantly depleted by photoevaporation. Thereafter the accretion rate declines exponentially (see equation 7), and it is thus the value of the e-folding time t_f (related to the viscous time-scale at R_t) which determines the time required for disc clearing, rather than the value of the photoevaporation rate. Consequently, secondary discs (with lower viscous time-scales at R_t) clear somewhat more rapidly than discs around primaries, even though they have lower photoevaporation rates. At larger separations, the inverse is true. The tidal boundary condition has less impact on the disc evolution and even at the later evolutionary stages when photoevaporation starts to become significant, the decline in disc surface density and accretion rate is close to the power-law decline in time (equation 4) for a freely expanding disc. Consequently, the level of the photoevaporative mass-loss is important in setting which disc clears first (i.e. the primary because of the higher photoevaporation rate).

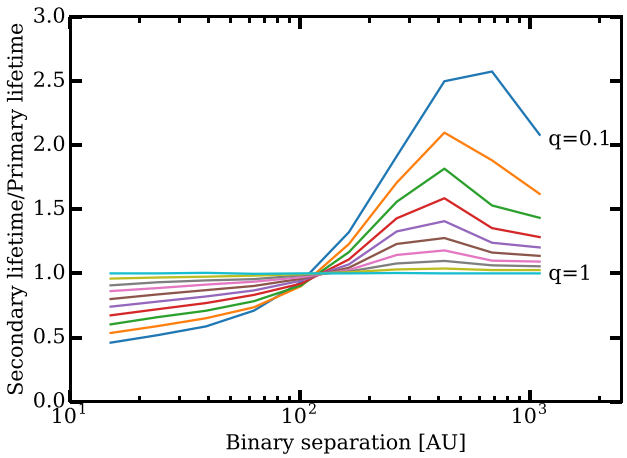

Figure 5. The ratio of the lifetime of the secondary to that of the primary (with a stellar mass of 1 $M_\odot$) as a function of binary mass ratio and separation, assuming that all stars follow the mean mass X-ray luminosity relation: $L_X = 2.3 \times 10^{30}(M_*/1M_\odot)^{1.44}$ erg s^{-1}. Discs around the secondary clear first for $a < 100$ au, whereas primaries clear first in wider binaries.

At large separations, the ratio of the secondary to primary lifetime tends to a limiting value that can be readily understood by considering the time at which the viscous accretion rate equals the photoevaporation rate. The latter is given by equation (4) so that (assuming that the initial disc mass scales with the stellar mass) we have $\dot{M} \propto M_* t^{-1.5}$. On the other hand $\dot{M}_X \propto L_X^{1.14} \propto M_*^{1.65}$ and hence one expects the disc lifetime to scale as $M_*^{-0.5}$. This is borne out by Fig. 5 (i.e. secondary lifetime roughly three times that of the primary for $q = 0.1$ at the largest separations). In this work, we assumed that the viscosity does not depend on the stellar mass. If the viscous time scales as $t_\nu \propto M_*^\beta$ (and hence the viscosity scales as $\nu \propto M_*^{-\beta}$, if the initial disc radius does not depend on the stellar mass as assumed in this paper), the scaling of the disc lifetime is modified as $M_*^{-0.5+\beta}$.

Fig. 5 represents the case that all stars have the average X-ray luminosity for their masses. If we instead adopt X-ray luminosities that are 1σ above (below), this average at all masses then the binary separation at which the primary and secondary lifetime is equal shifts to 70 and 240 au, respectively. This can be understood inasmuch as differential photoevaporation effects become more (less) important at higher (lower) X-ray luminosities.

4 DISCUSSION AND COMPARISON WITH THE OBSERVATIONS

We have investigated in the previous section how a disc in a binary evolves under the influence of viscosity and X-ray photoevaporation and now proceed to compare our model predictions with observations of young binaries. Our predictions of differential disc lifetimes need to be compared with *resolved* observations which can designate which member of the binary pair possesses a disc (Section 4.2). As in Section 3.2, in what follows we call systems in which both stars have discs as CCs, and those with a disc around the primary (secondary) only as CW (WC) systems. The reliable attribution of disc signatures to one component or the other is however observationally challenging, particularly for small separations and low-mass ratios. We therefore also make use (in Section 4.1) of the much larger data set of *unresolved* observations in which the presence of a disc cannot be attributed to a particular component but where it is only possible to distinguish the three classes above from a doubly disc-less (WW) system.

4.1 The reduced lifetimes of discs in binaries

In this section, we consider *unresolved* studies. Cieza et al. (2009) first reported a statistical difference in the separations of binaries with and without discs. Binaries without discs tend to have smaller separations, which can be explained if the disc lifetime is reduced in tight binaries. This initial finding has been confirmed by Kraus et al. (2012), who has shown in a sample of binaries in the Taurus-Auriga star-forming region that the disc fraction is a function of the binary separation. Tight binaries ($a < 40$ au) tend to have a smaller disc fraction than wide binaries, which instead have a disc fraction very similar to singles (∼80 per cent). From the arguments presented in Section 3, we expect this result since we have shown that the disc lifetime decreases with decreasing binary separation (see Fig. 4).

We can test this *quantitatively* by undertaking a population synthesis of discs. The goal is not to 'fit' the observations, but rather to test whether the same model that is able to reproduce the evolution of the disc fraction in singles can reproduce also the observations in binaries. We now assign to each primary a mass according to the Kroupa (2001) initial mass function (IMF). We then assign a mass to the secondary assuming a flat distribution in mass ratios, as found both in the solar neighbourhood (Raghavan et al. 2010) and in the Taurus star-forming region (Daemgen et al. 2015). We use the study of Raghavan et al. (2010) also to assign the separation, assuming a lognormal distribution in periods with an average of 10^5 d and a standard deviation of 2.28. We assign randomly X-ray luminosities to each star assuming a lognormal distribution with mean value $10^{30.37}$ erg s^{-1} and a scatter $\sigma = 0.65$, which is compatible with the observations in Orion of Güdel et al. (2007). We then scale the luminosity with $M_*^{1.44}$. For each model binary system, we designate the disc lifetime as the maximum of the lifetime of the primary's and secondary's disc.

In Fig. 6, we plot the resulting disc fraction for the binaries as a function of separation (blue points). To compute the fractions, we have assumed an age of Taurus of 2 Myr and binned the systems by separation. For comparison, we plot also as the horizontal line the disc fraction in singles from our models, which we have computed with a population synthesis with the same parameters (except that we do not use a closed boundary condition). The figure shows that wide binaries have a disc fraction similar to singles, although because the disc around the secondary for these separations is longer lived (Fig. 5) the disc fraction is actually slightly higher than in singles. Note that this effect is not visible in the observational data of Kraus et al. (2012), but it is not incompatible with this interpretation. For tight binaries, the disc fraction is reduced. As discussed in Section 3.1.2, this effect is mainly driven by the reduced viscous time at the outer boundary of the disc. The model predicts that the reduction in disc lifetime happens for a turnover separation of ∼50 au, which is consistent with the observations. For the tightest binaries ($a \sim 10$ au), the disc fraction reaches 10 per cent, which is less than the fraction of 25 per cent measured by Kraus et al. (2012). However, we notice that for these separations it is likely that the approximation that there is no circumbinary disc (which is longer lived for close separations; Alexander 2012) is probably no longer adequate. Moreover, the low number statistics of the observations means that there is considerable uncertainty in the measured fractions.

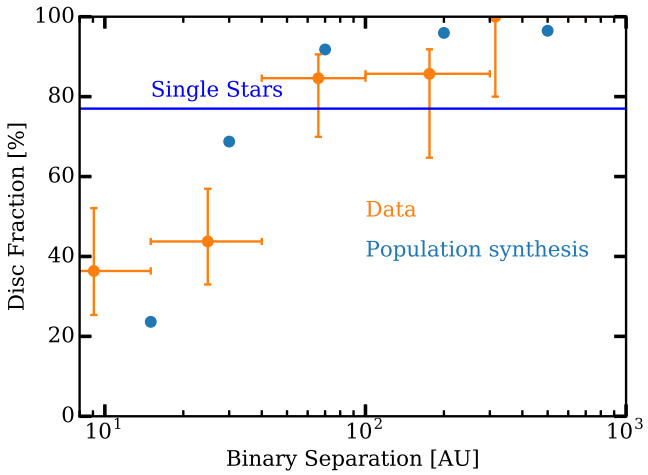

Figure 6. The fraction of binaries with a disc after 2 Myr in our population synthesis (blue points) as a function of the binary separations. For comparison, we plot also the data from Kraus et al. (2012) as the orange points with error bars. Wide binaries have a disc fraction slightly higher than singles (because the disc around the secondary is longer lived), whereas in tight binaries (i.e. $a \lesssim 50$ au) the disc fraction is significantly reduced due to the shorter viscous time.

It is interesting to note that, although the reduced disc lifetime at close separation is *mainly* a viscous effect, the inclusion of photoevaporation is still required to hasten further disc dispersal. To show this, we have run the same calculation again without including photoevaporation. We find that in this case no disc is completely dispersed at the age of Taurus. This might perhaps be cured by shortening the viscous time. As already stated, however, it is not our goal here to fit the observations performing a full investigation of the degeneracies between the parameters. We conclude that the model we have *assumed* as driver of disc evolution, where viscosity and X-ray photoevaporation are the driver of disc evolution, is broadly consistent with these observations.

4.2 Differential disc evolution in T Tauri binaries

In this section, we consider *resolved* studies. We have collected data from the literature using the catalogue of Monin et al. (2007) (Reipurth & Zinnecker 1993; Hearty et al. 2000; Köhler et al. 2000; Koresko 2002; Correia et al. 2006) and the new observations that have been taken since then (Comerón, Spezzi & López Martí 2009; Daemgen, Correia & Petr-Gotzens 2012; Daemgen et al. 2013). We have plotted the distribution of observed CCs, CWs and WCs in the plane of separation versus mass ratio in the left-hand panel of Fig. 7. To compute the mass ratios, we have converted spectral types to masses using the spectral-type-effective temperature scale of Hillenbrand & White (2004) and the pre-main-sequence tracks of Siess et al. (2000, assuming an age of 1 Myr). We do not plot WWs because the number of WWs relative to the other categories depends on the total length of time that stars spend as T Tauri stars, whereas the expected ratio of CWs and WCs to CCs can be directly inferred from the ratio of lifetimes.

In order to assess whether the observational results are compatible with the observations, we need to recall that we do not have information on the individual X-ray luminosities of the components in the observed binaries since the X-ray observations can only disentangle pairs separated by ∼1000 au (Preibisch et al. 2005; Güdel et al. 2007). Moreover, the numbers of objects observed is insufficient to be able to group the data as a function of primary mass, so that we cannot directly use a plot like Fig. 5 (which has a fixed primary mass and assumes that the X-ray luminosities of each component follow the mean X-ray luminosity as a function of stellar mass relationship). Instead, we here undertake population synthesis experiments: binary primaries are selected according to the IMF of Kroupa (2001), while X-ray luminosities are attached to each component by selecting from the same X-ray luminosity function used in the previous section. This is an important difference from the calculations reported in Section 3 because it is now possible, for example, for a secondary star to have a significantly higher X-ray luminosity than a primary star.

The model allows us to compute the expected fraction of systems that are CC, CW or WC. This fraction is a function of time (after

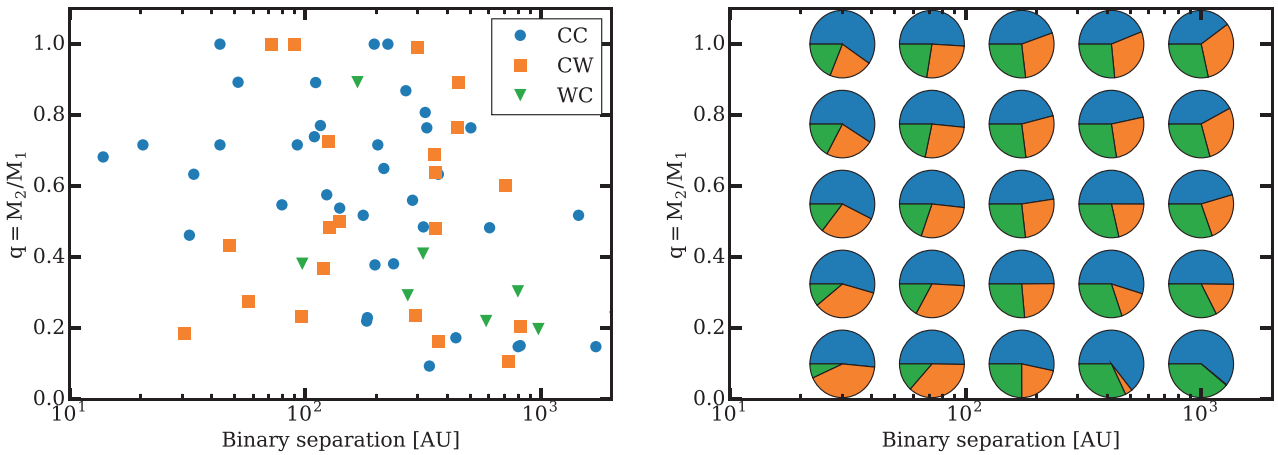

Figure 7. Comparison between observations and our models for the differential disc evolution in binaries. Left-hand panel: compilation of results from resolved observations. Blue circles are for CC systems, orange squares are for CW and green triangles are for WC. To place points in the plot, we have computed the mass ratio from the published spectral types using the spectral-type-effective temperature scale of Hillenbrand & White (2004) and the pre-main-sequence tracks of Siess, Dufour & Forestini (2000, assuming an age of 1 Myr). Right-hand panel: a montage of results from the Monte Carlo simulations showing pie charts of the relative times that the system spends as a CC, a CW or a WC as a function of binary separation (colours have the same meaning as in the left-hand panel: blue for CC, orange for CW and green for WC). Each pie chart contains objects with a range of primary masses. The plots illustrate that few WCs are expected at small separations while their incidence increases at large radii. For most of the parameter space, a mixture of CWs and CCs is expected.

enough time, all systems become WW); however, by assuming that we are sampling uniformly the distribution of stellar ages bearing discs, we can compute a time-averaged value (the situation is the same described in Rosotti et al. 2015 for the fraction of transition discs). This assumption is justified because the data with which we are comparing are a compilation of observations from different regions of different age.

In the right-hand panel of Fig. 7, we show a montage (as a function of binary separation and mass ratio) of the resulting fractions of systems which would be expected to be in the CC, CW and WC category. The colours have the same meaning as in the left-hand panel. At the closest separations, WCs are expected to be rare, particularly at low mass ratios (i.e. high $M_{\rm primary}/M_{\rm secondary}$): as discussed in Section 3, the differential evolution in tight binaries is driven mainly by the difference in viscous evolution time-scale and hardly at all by the differential levels of X-ray photoevaporation. For all mass ratios not equal to unity, the ratio of WCs to CWs increases with binary separation. The scatter in X-ray luminosities is important here. Whereas Fig. 5 (which assumes the mean mass X-ray luminosity relationship) suggests that *all* binaries at a separation of a few hundred A.U. should pass through a WC, rather than CW, phase, Fig. 7 shows that this is not the case: only for the most extreme mass ratios at large separations (lower right corner of the plot) no CW system is predicted, and for the regions of parameter spaces where the majority of mixed pairs are observed, the model predicts comparable numbers of CWs and WCs. This is not found in the observations, which find only a very limited number of WC systems. It is however likely that there is a selection bias against undertaking resolved studies on systems that turn out to be WCs: a faint excess around the secondary could be overlooked in unresolved studies, especially at small separations and low-mass ratios. Although we are unable to quantify this effect, we note that those WCs that have been observed tend to occupy the lower right area of parameter space which is where the model predicts that they should be more predominant.

The model also predicts a comparable abundance of CWs and CCs over most of the parameter space. This is compatible with the observations: in general no systematic difference between the blue and orange points can be observed. There are however two notable exceptions. The first is for systems with very small separations ($a \sim 30$ au) and mass ratios $q \gtrsim 0.4$. In this case, the model predicts an increase in the fraction of CCs, which seems to be confirmed by the relative lack of orange points in that region. The second concerns systems at large separations and small mass ratios, where the model predicts that there should be no CW system due to the much longer lifetime of secondaries. There are two CW data points with a separation of $\sim$800 au and a mass ratio below 0.2 that cannot be reconciled with the model. This could mean that the actual dependence of the disc lifetime with stellar mass is shallower than the one predicted by the model we employed. As discussed in Section 3.2, this is a consequence of the scaling of the viscous time with stellar mass that we assumed; a shallower scaling of the disc lifetime could be obtained by assuming that the viscous time mildly increases with the stellar mass, i.e. using the notation of Section 3.2, $0 < \beta < 0.43$. Given the small number of incompatible points, we will not discuss further this discrepancy. We stress however that the discrepancy highlights that this region of the parameter space with large separations and small mass ratio is ideal to study the dependence of the disc lifetime with the stellar mass, but the limited size of the current sample hinders further progress on the subject.

We conclude that the predictions of the model are compatible with the data available at the moment, provided that there is a significant bias against the detection of WC systems.

4.2.1 *The dependence of disc lifetime on stellar mass*

In our model, discs around isolated low-mass stars or low-mass stars in wide binaries are longer lived, which is the reason for the increased fraction of WC systems in the bottom right corner of Fig. 7. We have shown in this paper that this is compatible with the observations. The dependence of the disc lifetime on the stellar mass has many implications for understanding what kind of planetary systems may form around these stars. There is some indication from Kepler that the ratio of mass contained in planets to stellar mass is higher in low-mass stars (Mulders, Pascucci & Apai 2015) and an increased disc lifetime might provide an explanation for that.

We note that the dependence of disc lifetime with stellar mass has been studied in several other works. Most of them have used disc fractions deduced from the infrared (typically using *Spitzer*), subdividing stars in mass bins and then studying in which bin the disc fraction is lower (which is interpreted as evidence that discs are shorter lived). We note that this has produced contrasting results; while some studies have found that discs around low-mass stars are longer lived (e.g. Carpenter et al. 2006; Kennedy & Kenyon 2009; Ribas, Bouy & Merín 2015), the opposite result has also been claimed in the literature (Luhman et al. 2008, 2010). The differences can be probably ascribed to the different environmental conditions of the regions studied, as well as the difficulties in reaching completeness, which is essential for measuring disc fractions (this problem is particularly severe for low-mass, disc-less stars). With a different method, Ercolano et al. (2011) instead reached the conclusion that there is no systematic difference in the disc lifetime between low- and high-mass stars since there is no systematic difference between their spatial distribution. In this respect, we note that a possible explanation of their result is if the age spread in the region is lower than the disc lifetime. Finally, Kastner et al. (2016) recently analysed the stars in the TW Hya association, finding that a significant fraction of the stars later than mid-M still retain their disc, in contrast to the earlier spectral types. In addition, they found a decline in the ratio of X-ray luminosity to bolometric luminosity at late spectral types. Both these observational pieces of evidence are in agreement with our model.

We point out that binaries with wide orbits and low-mass ratios offer an additional way to study the dependence of the disc lifetime on the stellar mass. While the current constraints are limited due to the small size of the current sample of binaries, we note that binaries on wide orbits are observationally relatively easy to access. The fact that the primary is intrinsically brighter also mitigates the problem of finding a significant sample of low-mass stars. This is therefore a promising avenue for further studies.

4.3 Combining mass accretion rates and mass measurements

So far when comparing with observations, we have only considered if there is a disc or not, either in general in the binary (*unresolved* studies), or around a specific component (*resolved* studies). Observations are starting to provide more information, by measuring the mass of each individual disc (Harris et al. 2012; Akeson & Jensen 2014) and the accretion rate on each star (Daemgen et al. 2012, 2013). The additional information available places more constraints on the evolution of these discs; for example, resolved observations in the sub-mm have demonstrated (Jensen et al. 1996; Harris et al. 2012) that discs in binary systems have a lower mass than discs around single stars.

Rosotti et al. (2017, see also Jones, Pringle & Alexander 2012) have shown how measurements of disc masses and accretion rates can be combined through the dimensionless accretion parameter

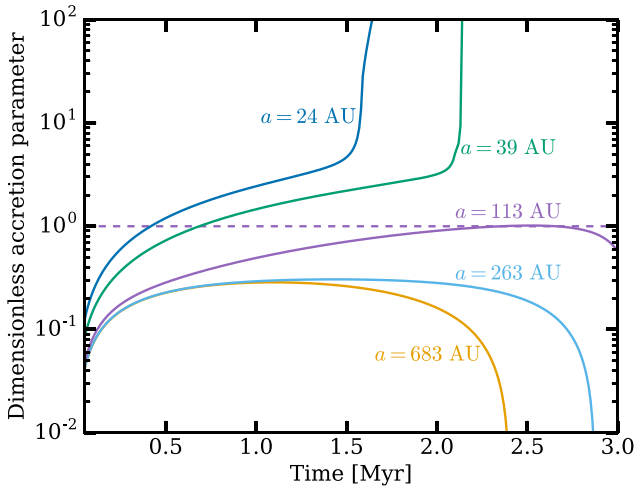

Figure 8. The evolution of the dimensionless accretion parameter in binaries with different separations (indicated on the plot). For illustrative purposes, we have chosen equal mass binaries with a mass of $1\,M_\odot$ with average X-ray luminosity. In wide binaries the parameter becomes significantly lower than unity due to the opening of a hole and the suppression of accretion on to the star; in close binaries the parameter is higher at all times, a factor of a few throughout most of the evolution and then increasing significantly during a short burst of accretion at the end as the disc is cleared from outside in.

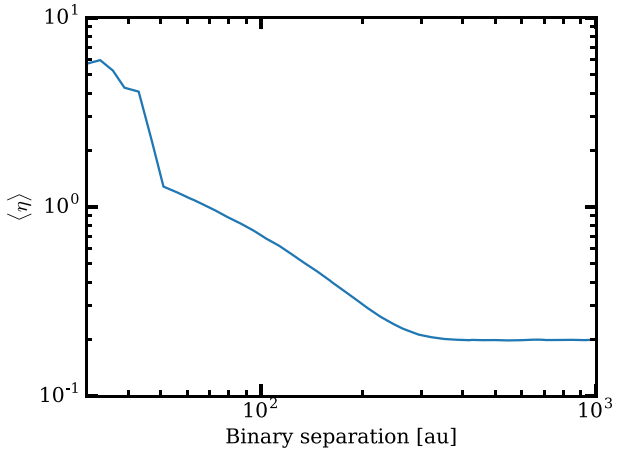

Figure 9. The dimensionless accretion parameter η, averaged over the disc lifetime, as a function of the binary separation.

$\eta = t\dot{M}/M_{\rm disc}$, where t is the age of the system. Fig. 8 shows the evolution in time of η in a binary system. For illustrative purposes, we have chosen equal mass binaries with a mass of $1\,M_\odot$ with average X-ray luminosity and a range of separations indicated on the plot. However, the qualitative behaviour we describe is general. The figure shows that for wide binaries (corresponding to the ones that form a hole, see Section 3.1.1), the evolution of η follows that expected for single stars that are eventually cleared by photoevaporation, i.e. η is of order unity for most of its evolution but declines steeply at late times during inside-out clearing. In close binaries, the accretion parameter instead increases monotonically with time, with a steep increase at late times during outside-in clearing. This behaviour is similar to the one in discs clearing under the effect of external photoevaporation. Thus, for the *same* disc mass, we expect close binaries to have a higher accretion rate (for most of the disc lifetime, of a factor 3–4).

To be more quantitative about the predicted change in the value of η in binaries, in Fig. 9 we plot η as a function of the binary separation. Because η is a function of time, we have averaged η over the disc lifetime. Observations sample disc at different phases of evolution and the time average can thus be compared with the distribution of η yielded by observations. The figure shows that there are three different regimes for η depending on the binary separation. The flat part of the curve at large separations ($a \gtrsim 300$ au) corresponds to discs that are dispersed before the outer radius has reached the tidal truncation radius. Disc evolution in these binaries proceeds as in single stars. Moving to closer separations, η increases monotonically as the binary separation is reduced. Binaries with an intermediate separation 50 au $< a <$ 300 au still clear from inside out (see Section 3.1) because of photoevaporation. However, because of the interaction with the outer boundary the accretion rate on to the star is enhanced, and thus η is a factor of a few higher than in single stars (for an example of the time evolution of η, see the $a = 113$ au case in Fig. 8). Finally, for very close binaries that experience outside-in clearing η greatly increases (more than a factor of 10).

To the best of our knowledge, there is currently no close binary system where both the disc mass and the accretion rate have been measured for individual components. Future observations will be able to test these theoretical predictions. There are already, however, observational implications as *unknown* binaries are likely present in many currently studied samples of T Tauri stars. This will affect the determination of the disc mass and of the accretion rate on to the stars. Manara et al. (2016) have shown observationally in the Lupus star-forming region the existence of a correlation between disc mass and accretion rate, which points to a constant value of η (approximately unity), consistent with disc evolution under the effect of viscosity. There is however a significant scatter of ~ 0.5 dex in the correlation. Here, we point out that the presence of binaries in the sample contributes to this observed scatter. In the case of a low-mass ratio $q \ll 1$, the primary will outshine the secondary so that the measured quantities (i.e. stellar mass, disc mass and mass accretion rate) will reflect the ones of the primary star. This will lead to an increase in the measured mass accretion rate with respect to a comparison sample of single stars. Contamination by binaries will therefore increase the scatter in the correlation. The same increase in scatter obviously happens for binaries where both stars contribute significantly to the flux and the impact of fitting their emission with a single stellar model is more difficult to quantify. We thus expect the correlation between disc mass and mass accretion rate to become tighter when binaries are removed from the sample.

4.4 Model limitations

Binaries are known to have a wide distribution of eccentricities (e.g. Raghavan et al. 2010), while in our model we have assumed that they are circular. Some discs in binaries are also observed to be misaligned to the binary orbital plane (e.g. Jensen & Akeson 2014). These two effects would cause some modification of the truncation radii but would not affect the conclusion that the secondary's disc is more truncated than the primary, with the possible exception of the most strongly misaligned systems (see e.g. Artymowicz & Lubow 1994; Pichardo et al. 2005 for works that included the effects of eccentricity and Lubow, Martin & Nixon 2015 for the effects of inclination). Another effect that we have

neglected in this paper is the possible truncation of the disc at the location of vertical resonances (Lubow 1981; Ogilvie 2002). However, the truncation happens only if the viscosity in the disc is low enough to be effectively in a so-called dead zone. Finally, probably the biggest uncertainty in our models is the mechanism responsible for driving accretion; while in this work we have assumed it is viscosity, recent work (e.g. Suzuki & Inutsuka 2009; Bai & Stone 2013; Fromang et al. 2013; Simon et al. 2013) is suggesting that winds might also play an important role by removing angular momentum from the disc. The effect of winds on disc evolution is however still poorly understood and for this reason we neglected it in this study. Even if accretion is driven by viscosity, there are still many associated unknowns, of which the most important from the perspective of this paper is its dependence on stellar mass.

5 CONCLUSIONS

Our calculations have modelled disc clearing by X-ray photoevaporation in a binary environment, capitalizing on the fact that the X-ray properties of young stars, the mass-loss profiles predicted by X-ray photoevaporation theory and the tidal truncation of discs within binary systems are all well-determined properties. The most poorly determined quantity that enters our models is the viscosity law in the disc. Here, we simply prescribe the viscosity as a power law of radius. While this allows a ready comparison with previous work, it should be borne in mind that this phenomenological description may not be a good approximation to the viscous properties of real discs.

Our results should be contrasted with those of Armitage et al. (1999, viscous only calculations in binary systems) and Owen et al. (2011, X-ray photoevaporation calculations in single stars). Our main results are as follows.

(i) We have shown that the sequence of disc clearing depends on the location of the disc's tidal truncation radius compared with the location of maximum X-ray photoevaporation (see Fig. 3). Except for the closest binaries (separations of a few au), a gap always opens as in the evolution around single stars. Inner holes form if the tidal truncation radius is well outside the region of maximum photoevaporative mass-loss (see Fig. 2). In this case, material remains in a ring outside the gap which is slowly eroded by photoevaporation while the inner disc drains. If however the disc is tidally truncated close to the maximum of photoevaporation (i.e. at a few tens of au) then the outer ring clears faster than the inner disc. Instead of forming an inner hole, we expect such discs to clear from the outside in. A consequence of this is that we should expect fewer transition discs (at least, of the type created by photoevaporation, see Owen & Clarke 2012) in binaries.

(ii) We have shown that in close binaries both discs see their lifetime reduced due to the smaller viscous time-scale. The quantitative predictions of the model compare well with the observations in the 2 Myr old Taurus star-forming region (Kraus et al. 2012).

(iii) We have shown that in closer binaries, discs tend to survive longer around the primary than the secondary component (see Fig. 5) due to the faster viscous time-scale induced by a smaller tidal truncation radius. The converse is true in wide binaries, where the differential evolution is instead driven by the higher mean photoevaporation rate in the case of the more massive (primary) component (i.e. on average discs survive for longer around the secondary). Since there is a scatter of X-ray luminosity at all masses, we expect a combination of WC/CW systems[5] for all separations, but with a preponderance of WC at large separations and of CW at small separations. Fig. 7 confirms that most WC systems are found at large separations. For the model to be compatible with the observations however we need to assume that there is a general, not yet quantified observational bias towards detecting WC systems (only few of which are known), justified by the difficulty of detecting infrared excess around the secondary due to the higher luminosity of the primary. With this assumption, the current observational data on the statistics of CC versus mixed pairs are broadly consistent with the predictions of the model.

(iv) Our model implies a longer lifetime for discs around low-mass stars; we note that this is consistent with, but poorly constrained from, the current observations. This is important to understand the process of planet formation around these stars. There is some indication from Kepler data that the ratio of mass contained in planets to stellar mass is higher in low-mass stars (Mulders et al. 2015) and the increased disc lifetime might provide an explanation. We point out that binaries on wide orbits and with low-mass ratios offer a way to study the dependence of the disc lifetime on the stellar mass, as an alternative to using disc fractions as a function of primary mass in star-forming regions. Binaries on wide orbits are observationally relatively easy to access, making this a promising avenue for further studies provided that the observational sample is expanded.

(v) Our population synthesis has allowed us to assess the relative lifetimes of primary and secondary discs in the regime of small separations where observational data is sparse (see Fig. 7). For example, we find that for binaries closer than 30 au and with $q < 0.5$, the primary's disc lifetime exceeds that of the secondary in the great majority of cases, a finding with implications for the relative incidence of planets around primary and secondary stars in binaries.

(vi) Future observations will provide another test of the models by combining measurements of both the mass accretion rate and the disc mass in the individual components of binary systems. Theoretically, we expect the dimensionless accretion parameter $\eta = t\dot{M}/M$ (Jones et al. 2012; Rosotti et al. 2017) to be a function of the binary separation, and is particular *higher* in close binaries (because of the shorter viscous time-scale imposed by the outer boundary) than in singles. Because *unknown* binaries likely contaminate existing observational samples, this effect increases the scatter in, for example, the correlation between disc masses and accretion rates reported by Manara et al. (2016). The scatter in the correlation was recently analysed by Lodato et al. (2017) and Mulders et al. (2017); both papers based their analysis on the fact that the magnitude of the observed scatter places constraints on the system age relative to the initial viscous time of the disc. A careful study of the sample to remove binaries would be needed to quantify how much unknown binaries contribute to this increased scatter.

ACKNOWLEDGEMENTS

We thank the referee for useful comments that improved the paper. We thank Sophie Kneller for her early work on the subject and Lisa Prato for giving us access to her observational data base of resolved binary observations. This work has been supported by the DISCSIM project, grant agreement 341137 funded by the European Research Council under ERC-2013-ADG, and by the Munich

[5] See Section 4 for a description of the classification C/W.

Institute for Astro- and Particle Physics (MIAPP) of the DFG cluster of excellence 'Origin and Structure of the Universe'.

REFERENCES

Akeson R. L., Jensen E. L. N., 2014, ApJ, 784, 62
Alexander R., 2012, ApJ, 757, L29
Alexander R. D., Armitage P. J., 2006, ApJ, 639, L83
Alexander R. D., Armitage P. J., 2007, MNRAS, 375, 500
Alexander R. D., Clarke C. J., Pringle J. E., 2005, MNRAS, 358, 283
Alexander R. D., Clarke C. J., Pringle J. E., 2006, MNRAS, 369, 229
Armitage P. J., Clarke C. J., Tout C. A., 1999, MNRAS, 304, 425
Artymowicz P., Lubow S. H., 1994, ApJ, 421, 651
Bai X.-N., Stone J. M., 2013, ApJ, 769, 76
Bath G. T., Pringle J. E., 1981, MNRAS, 194, 967
Carpenter J. M., Mamajek E. E., Hillenbrand L. A., Meyer M. R., 2006, ApJ, 651, L49
Cieza L. A. et al., 2009, ApJ, 696, L84
Clarke C. J., Gendrin A., Sotomayor M., 2001, MNRAS, 328, 485
Comerón F., Spezzi L., López Martí B., 2009, A&A, 500, 1045
Correia S., Zinnecker H., Ratzka T., Sterzik M. F., 2006, A&A, 459, 909
Daemgen S., Correia S., Petr-Gotzens M. G., 2012, A&A, 540, A46
Daemgen S., Petr-Gotzens M. G., Correia S., Teixeira P. S., Brandner W., Kley W., Zinnecker H., 2013, A&A, 554, A43
Daemgen S., Bonavita M., Jayawardhana R., Lafrenière D., Janson M., 2015, ApJ, 799, 155
Doyle L. R. et al., 2011, Science, 333, 1602
Drake J. J., Ercolano B., Flaccomio E., Micela G., 2009, ApJ, 699, L35
Dullemond C. P., Natta A., Testi L., 2006, ApJ, 645, L69
Dumusque X. et al., 2012, Nature, 491, 207
Ercolano B., Rosotti G., 2015, MNRAS, 450, 3008
Ercolano B., Bastian N., Spezzi L., Owen J., 2011, MNRAS, 416, 439
Fedele D., van den Ancker M. E., Henning T., Jayawardhana R., Oliveira J. M., 2010, A&A, 510, A72
Fromang S., Latter H., Lesur G., Ogilvie G. I., 2013, A&A, 552, A71
Gorti U., Hollenbach D., 2009, ApJ, 690, 1539
Güdel M. et al., 2007, A&A, 468, 353
Haisch K. E., Jr, Lada E. A., Lada C. J., 2001, ApJ, 553, L153
Harris R. J., Andrews S. M., Wilner D. J., Kraus A. L., 2012, ApJ, 751, 115
Hartmann L., Calvet N., Gullbring E., D'Alessio P., 1998, ApJ, 495, 385
Hatzes A. P., Cochran W. D., Endl M., McArthur B., Paulson D. B., Walker G. A. H., Campbell B., Yang S., 2003, ApJ, 599, 1383
Hearty T., Neuhäuser R., Stelzer B., Fernández M., Alcalá J. M., Covino E., Hambaryan V., 2000, A&A, 353, 1044
Hillenbrand L. A., White R. J., 2004, ApJ, 604, 741
Hillenbrand L. A., Bauermeister A., White R. J., 2008, in van Belle G., ed., ASP Conf. Ser. Vol. 384, Cool Stars, Stellar Systems, and the Sun. Astron. Soc. Pac., San Francisco, p. 200
Jeffries R. D., Littlefair S. P., Naylor T., Mayne N. J., 2011, MNRAS, 418, 1948
Jensen E. L. N., Akeson R., 2014, Nature, 511, 567
Jensen E. L. N., Mathieu R. D., Fuller G. A., 1996, ApJ, 458, 312
Jones M. G., Pringle J. E., Alexander R. D., 2012, MNRAS, 419, 925
Kastner J. H., Principe D. A., Punzi K., Stelzer B., Gorti U., Pascucci I., Argiroffi C., 2016, AJ, 152, 3
Kennedy G. M., Kenyon S. J., 2009, ApJ, 695, 1210
Köhler R., Kunkel M., Leinert C., Zinnecker H., 2000, A&A, 356, 541
Koresko C. D., 2002, AJ, 124, 1082
Kraus A. L., Hillenbrand L. A., 2009, ApJ, 704, 531
Kraus A. L., Ireland M. J., Hillenbrand L. A., Martinache F., 2012, ApJ, 745, 19
Kroupa P., 2001, MNRAS, 322, 231
Lines S., Leinhardt Z. M., Baruteau C., Paardekooper S.-J., Carter P. J., 2015, A&A, 582, A5
Lodato G., Scardoni C. E., Manara C. F., Testi L., 2017, MNRAS, 472, 4700
Lubow S. H., 1981, ApJ, 245, 274
Lubow S. H., Martin R. G., Nixon C., 2015, ApJ, 800, 96
Luhman K. L. et al., 2008, ApJ, 675, 1375
Luhman K. L., Allen P. R., Espaillat C., Hartmann L., Calvet N., 2010, ApJS, 186, 111
Lynden-Bell D., Pringle J. E., 1974, MNRAS, 168, 603
Manara C. F. et al., 2016, A&A, 591, L3
Marzari F., Thebault P., Scholl H., Picogna G., Baruteau C., 2013, A&A, 553, A71
Monin J.-L., Clarke C. J., Prato L., McCabe C., 2007, in Reipurth B., Jewitt D., Keil K., eds, Protostars and Planets V. Univ. Arizona Press, Tucson, AZ, p. 395
Mulders G. D., Pascucci I., Apai D., 2015, ApJ, 814, 130
Mulders G. D., Pascucci I., Manara C. F., Testi L., Herczeg G. J., Henning T., Mohanty S., Lodato G., 2017, ApJ, 847, 31
Ogilvie G. I., 2002, MNRAS, 331, 1053
Owen J. E., Clarke C. J., 2012, MNRAS, 426, L96
Owen J. E., Ercolano B., Clarke C. J., Alexander R. D., 2010, MNRAS, 401, 1415
Owen J. E., Ercolano B., Clarke C. J., 2011, MNRAS, 412, 13
Owen J. E., Clarke C. J., Ercolano B., 2012, MNRAS, 422, 1880
Palla F., Stahler S. W., 2000, ApJ, 540, 255
Papaloizou J., Pringle J. E., 1977, MNRAS, 181, 441
Pichardo B., Sparke L. S., Aguilar L. A., 2005, MNRAS, 359, 521
Preibisch T. et al., 2005, ApJS, 160, 401
Pringle J. E., 1981, ARA&A, 19, 137
Pringle J. E., Verbunt F., Wade R. A., 1986, MNRAS, 221, 169
Rafikov R. R., 2013, ApJ, 764, L16
Raghavan D. et al., 2010, ApJS, 190, 1
Reipurth B., Zinnecker H., 1993, A&A, 278, 81
Reipurth B., Clarke C. J., Boss A. P., Goodwin S. P., Rodríguez L. F., Stassun K. G., Tokovinin A., Zinnecker H., 2014, in Beuther H., Klessen R. S., Dullemond C. P., Henning T., eds, Protostars and Planets VI. Univ. Arizona Press, Tucson, AZ, p. 267
Ribas Á., Merín B., Bouy H., Maud L. T., 2014, A&A, 561, A54
Ribas Á., Bouy H., Merín B., 2015, A&A, 576, A52
Rosotti G. P., Ercolano B., Owen J. E., 2015, MNRAS, 454, 2173
Rosotti G. P., Clarke C. J., Manara C. F., Facchini S., 2017, MNRAS, 468, 1631
Siess L., Dufour E., Forestini M., 2000, A&A, 358, 593
Simon J. B., Bai X.-N., Armitage P. J., Stone J. M., Beckwith K., 2013, ApJ, 775, 73
Stassun K. G., Feiden G. A., Torres G., 2014, New Astron. Rev., 60, 1
Suzuki T. K., Inutsuka S.-i., 2009, ApJ, 691, L49
Thebault P., 2011, Celest. Mech. Dyn. Astron., 111, 29
van der Marel N., Verhaar B. W., van Terwisga S., Merín B., Herczeg G., Ligterink N. F. W., van Dishoeck E. F., 2016, A&A, 592, A126
Welsh W. F. et al., 2012, Nature, 481, 475
Williams J. P., Cieza L. A., 2011, ARA&A, 49, 67

This paper has been typeset from a TEX/LATEX file prepared by the author.